

## Research Article

Steffen Strebels\* and Cornelius Neumann

# Creating high contrast in virtual night driving

<https://doi.org/10.1515/aot-2018-0048>

Received September 18, 2018; accepted November 7, 2018; previously published online December 8, 2018

**Abstract:** The reproduction of glare scenarios in driving simulators is restricted by the limitations of conventional projector and display technology. In existing solutions, light sources are usually added to the optical path by combining common simulator technology with, for example, grids based on light-emitting diodes (LED). In this article, we introduce a new way to simulate glare sources on a common driving simulator back-projection screen using an additional projector and an additional reflective screen. In a first attempt, a concept with retroreflective sheets is proposed, and the requirements and current limitations of this setup are shown. Further development of the concept leads to an attempt with holographic diffusers. With an experimental setup based on the second concept, we aim to assess its feasibility, evaluate current challenges, and outline future requirements. The results show that it is possible to simulate a static glare scenario with correct geometrical conditions and headlights with luminances of about 100 000 cd/m<sup>2</sup>. Current limitations are an unbalanced color efficiency, the size and cost of available diffusers, and the black-level values and in-picture contrast of the used projector that cause an outshining of the environmental simulation.

**Keywords:** glare simulation; holographic diffuser; retroreflection; virtual night driving.

## 1 Introduction

Light conditions and contrast are an essential factor in recognition, visual performance, and safety of drivers in both nighttime and daytime driving because drivers gain approximately 90% of their information visually [1]. Glare

from oncoming traffic, or even self-glare during night driving, formed the subject of many research studies. In DIN 5340 [2], glare is defined as high luminance or luminance difference that triggers visual interference. There are two types of glare: discomfort and disability. Discomfort glare describes the subjective perception of glare, while disability glare is an objective, quantifiable reduction in visual performance. Common glare sources at night are headlights, brake lamps, and retroreflective traffic signs; during the day, a low-lying sun is a frequent source of glare.

Glare studies are essential to achieve a better understanding of the effects of light on human vision and perception especially in night driving under mesopic conditions. Therefore, necessary field tests are based on real vehicle lamps and usually take place on test tracks or in laboratories. Other more fundamental studies are conducted with static experimental setups, in which all necessary parameters, such as background luminance, spectral and spatial conditions, and target positions, can be adjusted.

All experimental setups are technically and economically limited to a small range of scenarios or an abstract representation of the glare scenario. Studies that require the dynamics and complexity of real traffic scenarios can only be conducted with significant effort and complex experimental designs, and glare studies in dangerous traffic scenarios are not recommendable. In contrast, driving simulators offer the potential to reproduce a wide range of possible traffic scenarios and to combine real vehicle hardware and vehicle simulation models with an environmental simulation.

### 1.1 Hardware limitations

The transfer of static or dynamic glare scenarios to a driving simulator remains a technical challenge, especially for the required luminance, contrast dynamics, and spatial resolution of light sources. For this case, the limitation of conventional display and driving simulator technology is obvious.

Glare sources during night driving occur typically in a small field-of-view (FOV) and in high local contrast to the environmental luminance. While typical environmental luminances at night are in the range of 0.1–10 cd/m<sup>2</sup>, oncoming headlights may reach values of up to 10<sup>4</sup>–10<sup>7</sup> cd/m<sup>2</sup>.

\*Corresponding author: Steffen Strebels, Dr. Ing. h.c. F. Porsche AG, Test and Validation, Porschestr. 911, 70187 Weissach, Germany, e-mail: steffen.strebels@porsche.de

Cornelius Neumann: Karlsruhe Institute of Technology, Light Technology Institute, Engesserstr. 13, 76131 Karlsruhe, Germany

Although modern projectors offer high dynamic contrast and sufficient resolution, the limitation in static contrast and the scattering of light on common projector screens make it impossible to display high brightness. The typical maximum luminance of projection systems is between 100 and 2000 cd/m<sup>2</sup> [3]. High-dynamic-range displays have also improved greatly in the recent years: contemporary maximum capabilities are approximately 4000 cd/m<sup>2</sup>, and peak luminances of 10 000 cd/m<sup>2</sup> can be expected in the future [4]. While this represents substantial progress, the level of brightness and realizable in-picture-contrast are both still the limiting factors for a realistic night driving simulation.

## 1.2 Existing approaches

Existing approaches mainly compensate those hardware limitations with either software-based or hardware-based methods. A software-based approach, proposed by Meyer, is to model and simulate the adaptation process of the driver's eye during glare scenarios in the graphical representation of the environmental simulation via tone mapping [5]. Other hardware-based methods combine traditional driving simulators with additional light sources. The simulation of a low-lying sun, for example, was realized by Bolling et al. [6] by mounting a halogen lamp in front of the simulator screen and investigating the effects of different degrees of worn windscreens. Another approach aimed to simulate the brightness of oncoming headlights: Hwang et al. [7] integrated an LED grid on top of a display-based simulator and combined both light paths via a beam splitter. Another hybrid system was introduced by Haycock et al. [8], combining traditional projectors with high-intensity LED panels. Here, the LED panels simulate oncoming headlights. They can be moved along the screen and allow spatial and brightness mapping of the simulation environment and glare sources.

Although these approaches have proven effective in simulating glare, they are usually appropriate only for a small range of possible scenarios. In this article, we aim to present two concepts that separate the visualization of the environment and the glare sources by efficiently using the light of an additional projector. In the following section, as introduced in Ref. [9], we present our concept of glare simulation and evaluate two methods for realization. The more promising option with holographic diffusers leads to an experimental setup, which is analyzed in Section 3, to assess its feasibility and outline challenges and future requirements.

## 2 Design of glare simulation

### 2.1 Approach

For a realistic and comparable simulation of glare scenarios in virtual night driving, the following requirements must be fulfilled:

1. To realize the required high contrasts on the screen, the simulation of the low-luminance environment and the high luminance of glare sources must be created in different ways.
2. To reach high luminances with modern projectors, methods for a highly efficient use of the available light are necessary.
3. White and colored glare sources, like oncoming headlights or traffic signs, have to be represented.
4. The illuminance  $E_v$  at the observer's eyes by glare sources in the simulation should be comparable to the illuminance under the same conditions in real traffic.
5. The use of an eyebox is necessary to achieve equal illuminances at both eyes.
6. The concept should be applicable to driving simulator dimensions with the usual short distances from observer to screen of  $1 \text{ m} < d_o < 5 \text{ m}$ .

Those requirements lead directly to the condition of equal luminances in simulation and reality. Consequently, the illuminated geometry of the glare source should be correct.

The basic design is shown in Figure 1. A back-projection system provides the environmental simulation. Glare sources are added to the scenario by an additional projector on the same side as the observer. The aim is to avoid scattering and reflect this additional light very efficiently to where it is needed: into the eyes of the driver inside the simulator.

To avoid parallax effects and distracting changes in the accommodation state of the driver's eyes due to the Mandelbaum effect [10], the image planes of the environmental simulation and the glare sources should be the same.

In the following sections, we evaluate two possible additional reflective layers. One is based on retroreflective particles and the other on a specific reflecting holographic diffuser.

### 2.2 Retroreflective particles

One way to achieve high reflectivity is to use partially reflective glass beads [11]. In this method, the retroreflective particles are randomly distributed with a specified density  $\rho$  onto the simulator screen.

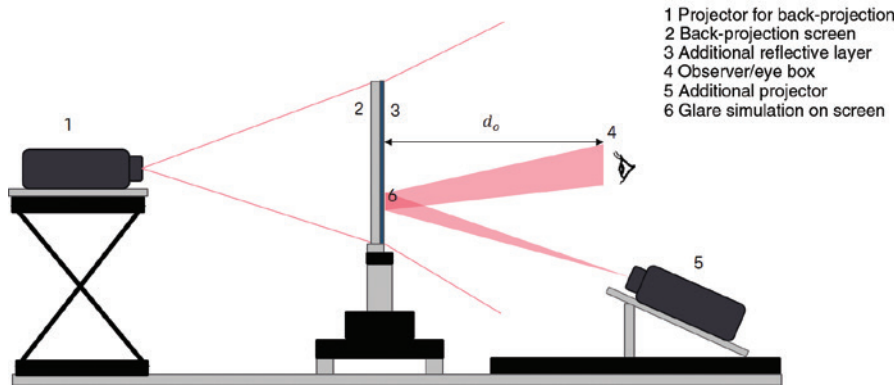


**Figure 1:** Basic design for creating high contrasts in virtual night driving via the combination of two light paths for the environment simulation (back) and glare sources (front).

The additional projector in the system only adds light to the scene where high luminances are needed. The resulting luminance depends on the variables given in the following equation, where  $\beta$  is the entrance angle, and  $E_{v,\perp}$  is the illuminance on the screen perpendicular to the incident light. Angle  $\alpha$  represents the observation angle, which is defined as the angle between the observer and the projector, and  $R_A$  is the coefficient of retroreflection.

$$L_v = \rho \cdot R_A(\alpha, \beta) \cdot \frac{E_{v,\perp}}{\cos(\beta)}$$

With presumed values of  $\rho = 0.1$  and an illuminance of 5000 lx, a minimum  $R_A$  of 200 cd/lx/m<sup>2</sup> is necessary to achieve luminances of approximately 10<sup>5</sup> cd/m<sup>2</sup>.

### 2.2.1 Evaluation and feasibility

To reach high luminances, it is essential to realize small observation angles in  $\alpha$  because of the strong dependence of  $R_A$  on  $\alpha$ . Common available retroreflective sheets, like those in Ref. [12], are usually optimized according to DIN 67520 [13] and are only efficient for  $\alpha < 1^\circ$  (Table 1).

In addition, the retroreflective particles must be designed in a way that avoids refraction of light from the

back projection. One possible method is to block light on the rear side of the particles. They must consequently be very small, and their density on the screen is limited due to the effects that they have upon the homogeneity and resolution of the driving simulator.

Because of the high efficiency in retroreflection, the projector must fulfill high requirements regarding the black-level values and in-picture contrast to avoid brightening the other areas on the screen. Furthermore, small movements of the observer's position relative to the projector have a large impact on the observation angle, especially if the distance to the simulator screen is small. This must be compensated by head tracking and adjustment methods or via a fixed observer position.

Apart from manufacturing a screen with retroreflective particles that fulfills the above requirements, the most significant feasibility issue with current available retroreflective sheeting is the required small observation angles. Figure 2 illustrates the relative distance  $d_r$  of the projector's focal point to the observer's focal point over their common distance  $d_o$  to the screen for  $\alpha = 0.33^\circ$ ,  $\alpha = 0.5^\circ$ , and  $\alpha = 1^\circ$ .

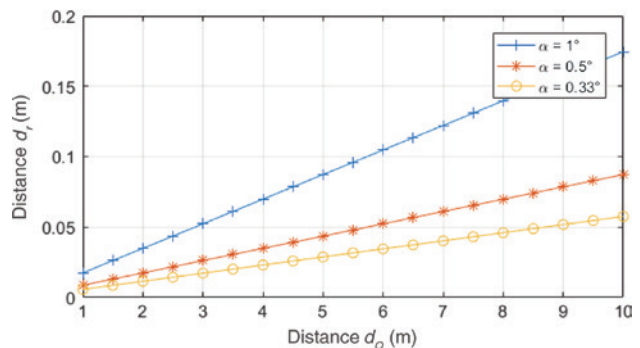


**Figure 2:** Relationship of the relative distance of the projector and observer and their common distance to the screen.

**Table 1:** Minimum  $R_A$  values of class RA2 retroreflective sheeting given in cd/lx/m<sup>2</sup> [13].

Observation angle $\alpha$	Entrance angle $\beta$		
	5°	30°	40°
0.2°	250	150	110
0.33°	180	100	95
2°	5	2.5	1.5

The resulting relative distances increase linearly with the distance to the screen. The necessary  $d_r < 0.05$  m for  $d_o < 5$  m is ergonomically unfeasible.

In addition, the design of an eyebox that allows an equal and homogeneous illuminance at both the observer's eyes is difficult to realize because of the proven high sensitivity of  $R_A$  to the observation angle at small distances.

Apart from methods to virtually decrease  $d_r$  with, for example, mirrors, solutions are to increase the distance, which restricts the usage in driving simulators. Another method is to change the reflectivity of the retroreflective particles to wider angles.

## 2.3 Holographic diffusers

The limitations of the previous concept led us to develop an approach that uses holographic diffusers [14]. It remedies the requirement for small observation angles, the eyebox, and the transmission of the back projection.

A holographic diffuser is a mainly transparent, photopolymer-based hologram, the reflection characteristic of which is in or near the plane of the holographic layer. In principle, the holographic diffuser represents a hologram of a diffusely scattering surface that is written in small pixels into the photopolymer. The angles of incidence and reflection can be set pixel by pixel. The convergence of the solid angles of each reflected ray defines the position and size of the resulting eyebox. The multiplexed pixels are wavelength specific, and red, green, blue (RGB) sensitive holograms can be made. Extensive literature exists on reflection holograms [15–17].

Depending on the exposure method, diffraction efficiencies can be higher than 40% on each of the three multiplexed wavelengths (RGB) for a full color holographic diffuser. With monochromatic diffusers, efficiencies of over 90% are possible [15]. The small spectral bandwidth of the diffuser sensitivity leads to high demands on the matching spectrum of the projector.

An estimation of the possible resulting luminance is more complex than that of retroreflective particles. It depends strongly on the spectrum of the projector  $\phi_{el}(\lambda)$ , the diffraction efficiency  $\eta(\lambda)$ , the effective area ( $A$ ) and its geometrical orientation as the polar angle  $\varepsilon$ , the spectral sensitivity of the human eye  $V(\lambda)$ , the photometric radiation equivalent  $K_m$  and the size of the chosen eyebox (implicit  $\Omega$ ), as the following equation demonstrates:

$$L_v = \frac{K_m \cdot \int_{380\text{ nm}}^{780\text{ nm}} \phi_{el}(\lambda) \cdot \eta(\lambda) \cdot V(\lambda) d\lambda}{A \cdot \Omega \cdot \cos(\varepsilon)}$$

With a presumed eyebox of 120 mm × 60 mm at a 1-m distance ( $\Omega \approx 0.0070$  sr) and an efficiency that results in 20% use of a presumed available illuminance of 5000 lx, luminances of approximately  $10^5$  cd/m<sup>2</sup> can be estimated.

### 2.3.1 Evaluation and feasibility

In contrast to retroreflective particles, the reflection characteristic of the holographic diffuser pixels can be designed in a way that results in a sufficiently and homogeneously illuminated eyebox.

By using an RGB hologram and a projector matching its wavelength sensitivity, after color calibration, one can depict white and defined colored glare sources, such as traffic signs or brake lights. In addition, the depiction of glare sources with different geometries, such as the Porsche four-point headlight (Figure 3), is possible.

The effects of a possible small fraction of absorption of the back projection can be alleviated by a luminance calibration that results in a slightly brighter display of the environmental simulation.

However, due to the limitations in the efficiency of the diffuser, light from the front projection brightens the back-projection screen at the source of the glare. This can also be resolved by a luminance calibration and results in a lookup table that assigns projector pixel values with the resulting luminances. Another issue is that the black-level values of the projector may lead to an outshining of the environmental simulation. For this reason, the projector needs to fulfill high requirements in its black-level value presentation and in-picture contrast.

One must also consider that holograms based on photopolymers may work from both sides. In simulating and designing the diffuser, the diffraction of the scattering light of the back projection has to be minimized. Finally,



**Figure 3:** Porsche Panamera Turbo (type G2) with four-point headlights [18].



a practical limitation for this setup is the current cost and limited size of the holographic diffusers.

Overall, this is a promising method for glare simulation, and in the following section, an experimental test setup is shown to examine its feasibility.

## 3 Evaluation of the holographic concept

### 3.1 Experimental setup

The holographic diffuser used for the experimental setup had dimensions of 195 mm×130 mm and consisted of 16 RGB-multiplexed pixels per square millimeter. The normalized diffraction efficiencies are shown in Figure 4.

Our diffuser was designed with a projector tilted by 5° to the perpendicular axes of the screens and positioned at a projection distance of approximately 0.45 m.

In this configuration, the resulting eyebox was maximal in size and homogeneity. It had a size of 30 mm×60 mm, at a distance of approximately 0.5 m and tilted by 50° to the perpendicular axes of the screens. For evaluation, a luminance camera 5 color (LMK) of Techno Team (TechnoTeam Bildverarbeitung GmbH, Illmenau, Germany) and a neutral density filter from Haidaa-Deutschland, Geesthacht, Germany (Slim Pro II, ND3.0, 1000×) were positioned in the middle of the eyebox position. The experimental setup is illustrated in Figure 5.

The projector used to provide glare sources is an Optoma W304M (Optoma Deutschland GmbH, Dusseldorf, Germany) DLP projector with a specific contrast of 1:10 000, a luminous flux of 3100 lm, and a common high-pressure lamp, all of which were used to obtain the measured spectrum in Figure 4. For back projection, an Epson EH-TW6100 (Epson Deutschland GmbH, Meerbusch, Germany) with 2300 lm and a contrast ratio of 1:40 000 was used.

The mounted screen was a Barco300 (Barco Deutschland GmbH, Kalsruhe, Germany) back-projection screen with a peak gain

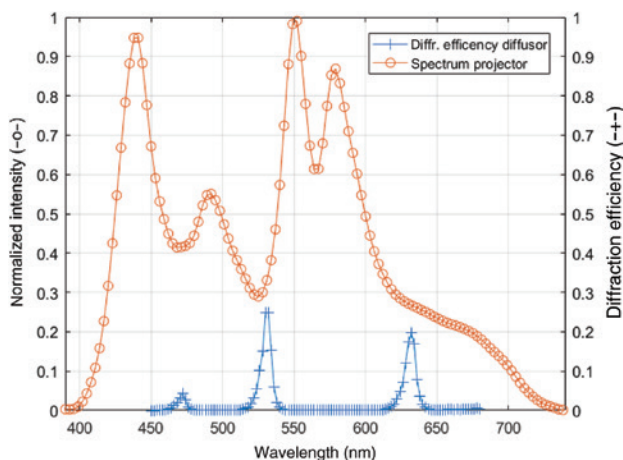


**Figure 4:** Normalized spectrum of the projector used for the simulation of glare sources and the corresponding diffraction efficiency of the holographic diffuser.

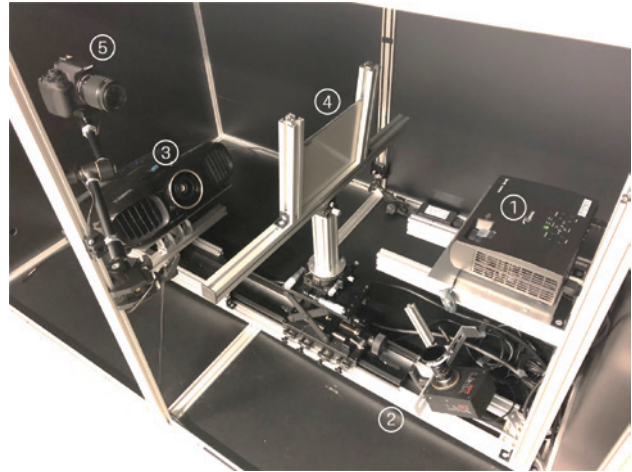


**Figure 5:** Photograph of the experimental test setup with front projection (1), luminance camera (2), back projection (3), back-projection screen and holographic diffuser (4), and camera for calibration (5).

of 0.3 and half gain at 70°. For easier handling and use in different test setups, the holographic diffuser was attached to a 3-mm-thick glass plate, which was positioned next to the back-projection screen. The resulting distance of both screens was 3 mm.

The experimental setup was constructed in a closable box, and all parts were controllable from the outside to minimize interfering illumination effects.

The diffuser, as displayed in Figure 4, had unequal diffraction efficiencies in RGB. Without color calibration, the resulting picture had a green cast. However, we renounced color calibration because it would have led to an alignment with the blue color efficiency that was about 20% of the green one and would have, therefore, caused a severe loss in possible luminance. As demonstrated in Ref. [14], holographic diffusers with equal diffraction efficiencies are possible, and investigations with balanced colors are the focus of the next test setups.

A more advanced projector than the Optoma used in the experiment would be a laser projector with a perfectly matching spectrum. However, the goal was to assess the feasibility of visualizing a static scene representing an oncoming car with correct glaring luminances and geometrical dimensions. For this investigation, the test setup was sufficient.

### 3.2 Calibration

To obtain a distortion-free projection and to allow valid statements for a photometric evaluation, we needed to intrinsically and extrinsically calibrate all projectors and cameras. The intrinsic calibration for the LMK was based on Zhang's method [19], and the intrinsic calibration for both projectors was conducted with the procedure introduced by Moreno and Taubin [20]. To maximize the accuracy, a Canon EOS 700D (Canon Deutschland GmbH, Krefeld, Germany) single-lens reflex camera for the projector calibration was used.

With an extrinsic calibration, based on the method of Falcao et al. [21], the relative coordinates and orientation of each device could be gained, and projections without distortion were possible.

**Table 2:** Reprojection error of the intrinsic and extrinsic calibration of the projector and luminance camera.

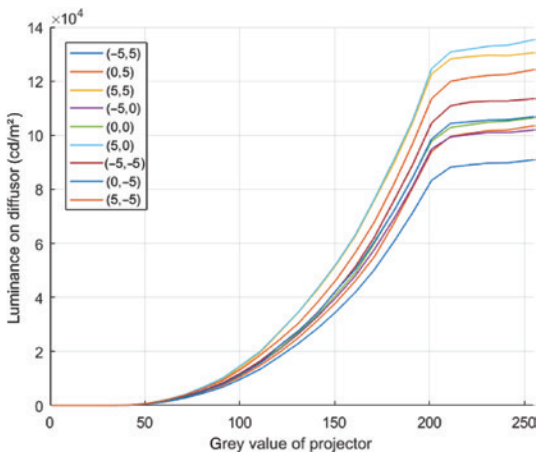
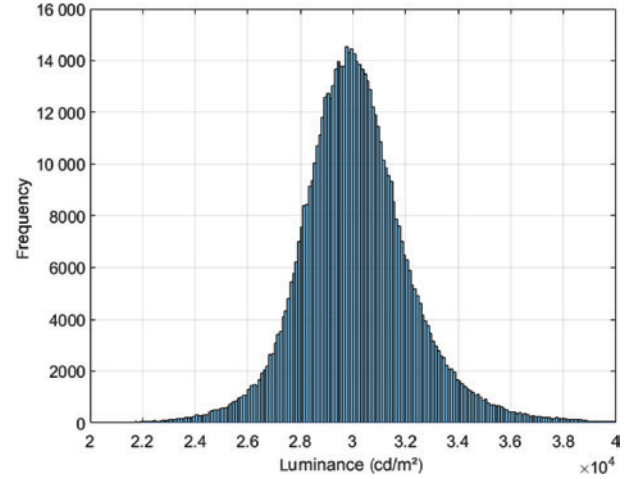
[Pixels]	SD in x	SD in y	ME in x	ME in y
Optoma	0.076	0.116	0.26	0.4
Epson	0.26	0.42	0.7	1.4
LMK	0.26	0.33	1.8	2.6
Back projection (extrinsic)	0.35	0.20	0.5	0.7
Front projection (extrinsic)	0.15	0.39	0.35	0.7

Table 2 shows the reprojection error in standard deviation (SD) and maximum error (ME) in x and y in pixels.

With the gained exact geometrical model, we could merge the front and back projections. The back projection is visualized with the Virtual Test Drive (VTD) [22] as an environmental simulation. For the visualization of oncoming vehicles, we implemented a Computer-Aided-Design (CAD)-based model of a Porsche Panamera (type G2), which is the same vehicle as that used in comparing measurements in our light lab in the next section. In this article, only static night driving scenes are considered, and real-time rendering was not implemented. The virtual observer position and perspective of the rendered environment can be set in the VTD image generator. By application of a post-processing step and using the results of the calibration above, a distortion-free view is possible.

To add the correct luminances of the glare sources via the front projection, a luminance calibration was needed. For calibration, we mapped each  $3 \times 3$ -pixel square of the Optoma projector to the corresponding luminances. Figure 6 highlights the matching of nine example pixels after interpolation.

With this method, effects such as hotspots and inhomogeneous areas could also be compensated. Other effects, such as local fluctuations in the efficiency of single pixels, were not considered. Figure 7 exhibits the local fluctuation in a histogram for a target luminance of  $30\,000\text{ cd/m}^2$  after calibration. The median value is  $29\,970\text{ cd/m}^2$ . The local fluctuations are also visible in the linear scaled luminance picture of the homogenous area of the left headlight in Figure 8. More detailed investigations to quantify the fluctuations are part of future work.

**Figure 6:** Matching of gray values of the projector to corresponding luminances depending on their coordinates (x,y) in centimeters on the holographic diffusor, where the coordinate origin (0,0) corresponds to the center of the diffusor.**Figure 7:** Histogram of the fluctuation of luminances at a target luminance of  $30\,000\text{ cd/m}^2$  after calibration, measured on the full diffuser area.

The results demonstrates that glare sources with luminances between  $90\text{ cd/m}^2$  and over  $100\,000\text{ cd/m}^2$  could be displayed in this test setup. The lower luminances caused by the black values of the projector resulted in an outshining of the environmental simulation.

### 3.3 Headlight simulation

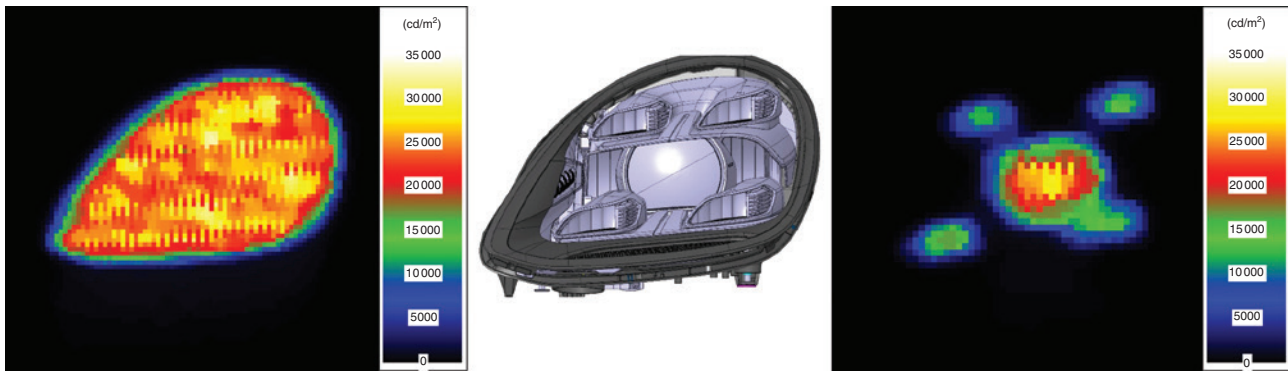
Using displayable luminances of up to  $100\,000\text{ cd/m}^2$ , one could simulate oncoming headlights with a low beam. The oncoming headlight can be modeled with real geometrical proportions in two different ways. One uses only the outer contour of the headlight and, therefore, allows the display of lower target luminances. The other, more realistic way models the visible luminous geometry and reproduces the real characteristics of a headlight. Figure 8 shows both cases.

The target luminance was calculated by the following equation, in which  $I_v$  corresponds to the goniophotometrically measured luminous intensity of the headlight and  $A$  to the corresponding area of the light source:

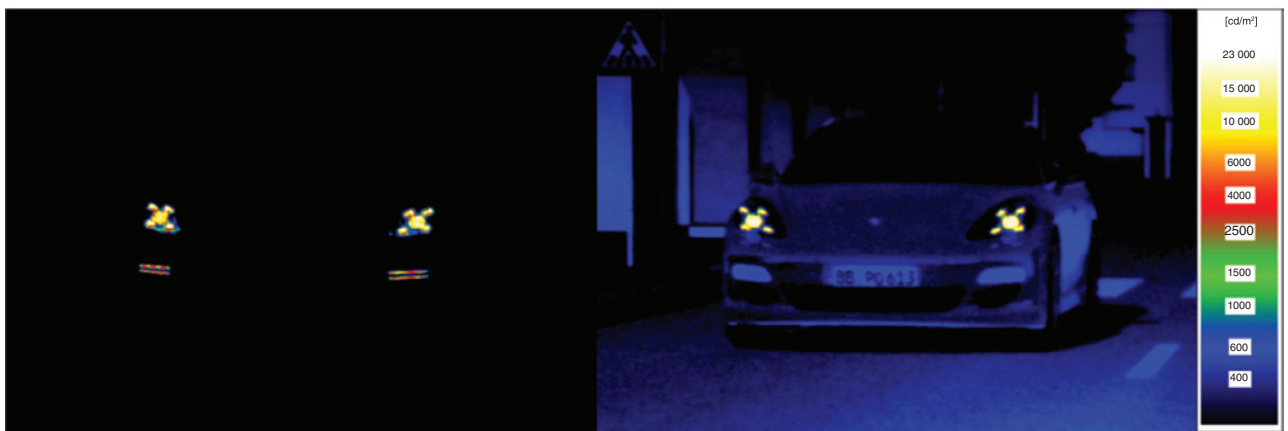
$$L_v = \frac{I_v}{A \cdot \cos(\varepsilon)}$$

Figure 8 reveals that at the transitions from high to low luminances, the projector was unable to display locally high in-picture contrasts. The transitions appear to be blurred. This caused inaccuracy in the resulting glare illumination at the observer's eye, and the local fluctuations are also clearly evident. Also a double-image of the headlight is slightly visible, caused by the 3 mm distance of diffusor and back-projection screen.

A sample application of the test setup is shown in Figure 9. The left image depicts a luminance measurement of an oncoming Porsche Panamera in our light lab. The relative distances of the LMK and the left headlight focus point are  $(x, y, z) = (20\text{ m}, 1.5\text{ m}, 0.4\text{ m})$ . The background is too dark ( $0\text{--}2\text{ cd/m}^2$ ) to be visible in the logarithmically scaled luminance picture. The static scene was reproduced in VTD with the same relative distances and perspective. The distortion and luminance got rendered according to the calibration models. The brightness of the environmental simulation is raised to approximately  $450\text{ cd/m}^2$  to counter the outshining caused by the front



**Figure 8:** Representation of the real CAD headlight geometry (center) on the holographic diffuser as a model of the contour (left) or the luminous geometries (right). Both are depicted on a linear scale with a target luminance 30 000 cd/m<sup>2</sup>.



**Figure 9:** Static luminance measurement of a real vehicle (left) and an experimental setup with a holographic diffuser (right) of an oncoming Panamera (type G2) with low beam at about 20-m distance. Both depicted on a logarithmic scale.

projection and to validate the geometrical calculations. The luminance of the four-point headlight was simulated correctly.

### 3.4 Conclusion

According to these results, it is possible to simulate high luminances and complex glare geometries. The presented method of using multiplexed holographic diffusers for an additional light path and the display of glare sources is partially effective, but also requires further investigation.

The most significant limitation of the test setup is the use of a common projector. Improvements are necessary in matching the spectrum with the diffuser. This is possible with laser projectors.

Assuming that the brightness of the environmental simulation for night driving needs to display realistic luminances in the range of  $10^{-1}$ – $10^1$  cd/m<sup>2</sup> and maximum luminances of roughly  $10^6$  cd/m<sup>2</sup>, a high in-picture contrast is needed. If black pixel values must only cause 1% of the additional brightness of the environmental simulation, an in-picture contrast of over 1:1 000 000 000 is necessary. For lower maximum luminances or higher minimum luminances, this requirement accordingly decreases. In addition, high locally in-picture contrast is needed, to reduce blurring in the areas in which the glare sources transition.

The high demand in the provided luminous flux decreases if the projection can be dynamically adjusted to the occurring glare source. Glaring objects only occur in a small FOV, and therefore, methods that avoid the projection of any black values on the screen must be investigated. Overall, these demands specify a projector that is currently not available, and further research is needed.

The limitations caused by the holographic diffuser are remediable, especially the equal color representation. To achieve even higher efficiencies, the stacking of three monochromatic RGB diffusers can be tested.

## 4 Summary and outlook

In this paper, two different concepts for creating high contrasts through an additional optimized optical path were presented. First, a method based on retroreflective particles was conceptualized and evaluated. The current limitations revealed by this technique led to an approach with holographic diffusers. In an experimental setup, a system based on the holographic concept with back- and



additional front projection was built. After a geometric and luminance calibration, we simulated a static glare scenario of an oncoming vehicle at low beam with the Porsche four-point light. We demonstrated the feasibility of simulating glare sources of up to 100 000 cd/m<sup>2</sup>.

Current limitations are the size and cost of holographic diffusers, as well as projectors that enable in-picture contrast of 1:1 000 000 000, to avoid unintended brightened areas on the screen.

In an ongoing work, investigations are planned with a newly designed diffuser. We aim to achieve a more balanced color diffraction efficiency, an orthogonal observer position, and a wider eyebox at a greater viewing distance. A stacking of three diffusers with monochromatic designs, instead of multiplexing, must also be investigated. In addition, physiological studies with test subjects have to be done to ensure a realistic appearance. The results will lead to further development of the diffuser-based concept.

## References

- [1] D. Shinar, E. D. McDowell and T. H. Rockwell, *Hum. Factors* 19, 63–71 (1977).
- [2] DIN 5340:1998-04, ‘Terms for Physiological Optics’, (1998).
- [3] L. Luz and B. Doshier, in ‘Visual Psychophysics: From Laboratory to Theory’, (MIT Press, Cambridge, USA, 2013).
- [4] C. Chinnock, in ‘Dolby Vision and HDR10’, (White Paper of Insight Media, Norwalk, USA, 2016).
- [5] B. Meyer, in ‘Measuring, Modeling and Simulating the Re-adaptation Process of the Human Visual System After Short-Time Glares in Traffic Scenarios’, (TU Braunschweig, Dissertation, 2015).
- [6] A. Bolling, G. Sørensen and J. Jansson. in ‘Proceedings of the DSC Europe’, pp. 23–31 (2010).
- [7] A. D. Hwang and E. Peli, in ‘3rd International Conference on Road Safety and Simulation’, Indianapolis, USA (2011).
- [8] B. Haycock, N. Koenraad, M. Potter and S. Advani, ‘Proceedings of the DSC Europe’, pp. 77–84 (2016).
- [9] S. Strebel and C. Neumann, in ‘Proceedings of the DSC Europe’, pp. 151–155 (2018).
- [10] C. Neumann and S. Strebel, Patent specification: Nr. DE102017204435A1, (2017).
- [11] D. A. Owens, *J. Opt. Soc. Am.* 69(5), 646–652 (1979).
- [12] Orafol Europe GmbH, ORALITE® 5810 High Intensity Grade, Technical Datasheet, (2018).
- [13] DIN 67520:2013-10 Retro-reflecting materials for traffic safety – Photometric minimum requirements for retro-reflective sheetings, (2013).
- [14] S. Miemietz, S. Strebel and Y. Chamseddine, Patent specification: Nr. DE102017204350B3, (2017).
- [15] M.-L. Piao, K.-C. Kwon, H.-J. Kang, K.-Y. Lee and N. Kim, *Appl. Opt.* 54, 5252–5259 (2015).
- [16] M. Schmiedchen, *Modellbildung und Realisierung von Holografischen Aufprojektionsflächen* (TU Darmstadt, Dissertation, 2005).
- [17] B. S. Meyer, *Holographie in der Display Technologie*, (Karlsruhe Institut für Technologie, Dissertation, 2015).
- [18] Porsche AG, Porsche VM Mediendatenbank, <https://vmmedia.porsche.de/>, accessed 29.10.2018.
- [19] Z. Zhang, in ‘Proceedings of the Seventh IEEE International Conference on Computer Vision, Kerkyra, Greece, vol. 1, pp. 666–673 (1999).
- [20] D. Moreno and G. Taubin, in ‘Second International Conference on 3D Imaging, Modeling, Processing, Visualization and Transmission’, Zurich, Switzerland, pp. 464–471 (2012).
- [21] G. Falcao, N. Hurtos, J. Massich and D. Fofi, *Projector-Camera Calibration Toolbox*, <http://code.google.com/p/procamcalib>, (2009).
- [22] Vires Simulationstechnik GmbH, *Virtual Test Drive, User Manual O*, (2017).



**Steffen Strebel**

Dr. Ing. h.c. F. Porsche AG, Test and Validation, Porschestr. 911, 70187 Weissach Germany  
[steffen.strebel@porsche.de](mailto:steffen.strebel@porsche.de)

Steffen Strebel received his MSc degree in Engineering Cybernetics from the University of Stuttgart in 2015. Since then, he is employed at the Dr. Ing. h.c. F. Porsche AG in the Department of Test and Validation. In 2016, he started his PhD at the Light Technology Institute at the Karlsruhe Institute of Technology (KIT). His current research focuses on concepts for functional tests and simulation of automotive lighting systems.



**Cornelius Neumann**

Karlsruhe Institute of Technology, Light Technology Institute, Engesserstr. 13  
 76131 Karlsruhe, Germany

Cornelius Neumann studied Physics and Philosophy at the University of Bielefeld, Germany. After his PhD, he worked for the automotive supplier Hella in the advanced development for automotive lighting. During his time at Hella, he was responsible for signal lighting, LED application, and acted as a director of the L-LAB, a laboratory for lighting and mechatronics in public–private partnership with the University of Paderborn, Germany. In 2009, he became Professor for Optical Technologies in Automotive and General Lighting and one of the two directors of the Light Technology Institute at the Karlsruhe Institute of Technology, Germany.